



The Effects of PMMA on Ballistic Impact Performance of Hybrid Hard/Ductile All-Plastic- and Glass-Plastic-Based Composites

**by Alex J. Hsieh, Daniel DeSchepper, Paul Moy, Peter G. Dehmer,
and John W. Song**

ARL-TR-3155

February 2004

NOTICES

Disclaimers

The findings in this report are not to be construed as an official Department of the Army position unless so designated by other authorized documents.

Citation of manufacturer's or trade names does not constitute an official endorsement or approval of the use thereof.

Destroy this report when it is no longer needed. Do not return it to the originator.

Army Research Laboratory

Aberdeen Proving Ground, MD 21005-5069

ARL-TR-3155**February 2004**

The Effects of PMMA on Ballistic Impact Performance of Hybrid Hard/Ductile All-Plastic- and Glass-Plastic-Based Composites

Alex J. Hsieh, Daniel DeSchepper, Paul Moy, and Peter G. Dehmer
Weapons and Materials Research Directorate, ARL

John W. Song
Natick Soldier Center

Report Documentation Page			Form Approved OMB No. 0704-0188		
<p>Public reporting burden for this collection of information is estimated to average 1 hour per response, including the time for reviewing instructions, searching existing data sources, gathering and maintaining the data needed, and completing and reviewing the collection information. Send comments regarding this burden estimate or any other aspect of this collection of information, including suggestions for reducing the burden, to Department of Defense, Washington Headquarters Services, Directorate for Information Operations and Reports (0704-0188), 1215 Jefferson Davis Highway, Suite 1204, Arlington, VA 22202-4302. Respondents should be aware that notwithstanding any other provision of law, no person shall be subject to any penalty for failing to comply with a collection of information if it does not display a currently valid OMB control number.</p> <p>PLEASE DO NOT RETURN YOUR FORM TO THE ABOVE ADDRESS.</p>					
1. REPORT DATE (DD-MM-YYYY) February 2004		2. REPORT TYPE Final		3. DATES COVERED (From - To) June 2002–August 2003	
4. TITLE AND SUBTITLE The Effects of PMMA on Ballistic Impact Performance of Hybrid Hard/Ductile All-Plastic- and Glass-Plastic-Based Composites			5a. CONTRACT NUMBER		
			5b. GRANT NUMBER		
			5c. PROGRAM ELEMENT NUMBER		
6. AUTHOR(S) Alex J. Hsieh, Daniel DeSchepper, Paul Moy, Peter G. Dehmer, and John W. Song*			5d. PROJECT NUMBER H84		
			5e. TASK NUMBER		
			5f. WORK UNIT NUMBER		
7. PERFORMING ORGANIZATION NAME(S) AND ADDRESS(ES) U.S. Army Research Laboratory ATTN: AMSRD-ARL-WM-MA Aberdeen Proving Ground, MD 21005-5069			8. PERFORMING ORGANIZATION REPORT NUMBER ARL-TR-3155		
9. SPONSORING/MONITORING AGENCY NAME(S) AND ADDRESS(ES)			10. SPONSOR/MONITOR'S ACRONYM(S)		
			11. SPONSOR/MONITOR'S REPORT NUMBER(S)		
12. DISTRIBUTION/AVAILABILITY STATEMENT Approved for public release; distribution is unlimited.					
13. SUPPLEMENTARY NOTES * U.S. Army Soldier and Biological Chemical Command, Soldier Systems Center, Natick Soldier Center, Natick, MA 01760-5019					
14. ABSTRACT The U.S. Army Research Laboratory is focusing on utilizing the materials-by-design strategy in the development of transparent armor systems to achieve lightweight, mobility, enhanced survivability, and lower life cycle costs for the soldiers and ground vehicle protection. The focus of this research is to identify the material parameters that are critical for the ballistic performance of hybrid hard/ductile laminate systems. We evaluated the role of poly(methyl methacrylate), (PMMA), on the impact response of composites consisting of PMMA and polycarbonate, (PC), as well as on the PC-Glass-PMMA-PC laminates against the .22-cal. fragment simulator projectile and the 124-gr 9-mm projectile. Increasing the thickness of PMMA improved the overall impact capability of these laminates. Incorporation of PMMA as an intermediate ply between the glass and ductile PC appeared to be a very effective approach for the design of glass-plastic laminates. We attributed this observation to the high strain-rate sensitivity characteristics of the monolithic PMMA. Preliminary results obtained from the 9-mm projectile testing clearly indicated that the PMMA-based all-plastic laminates maintained a significant amount of residual visibility after impact, which was critical for transparent armor applications.					
15. SUBJECT TERMS ballistic measurements, poly(methyl methacrylate), PMMA, polycarbonate, PC, PMMA-PC laminates, glass-plastic laminates					
16. SECURITY CLASSIFICATION OF:			17. LIMITATION OF ABSTRACT UL	18. NUMBER OF PAGES 26	19a. NAME OF RESPONSIBLE PERSON Alex Hsieh
a. REPORT UNCLASSIFIED	b. ABSTRACT UNCLASSIFIED	c. THIS PAGE UNCLASSIFIED			19b. TELEPHONE NUMBER (Include area code) 410-306-0698

Contents

List of Figures	iv
List of Tables	v
Acknowledgments	vi
1. Introduction	1
2. Experimental	2
2.1 Target Materials	2
2.2 Ballistic Testing.....	3
2.3 Compression Measurements.....	4
3. Results and Discussion	5
3.1 PC-PMMA-PC vs. PC-PC-PC Laminates.....	5
3.2 Effect of PMMA Plate Thickness	7
3.3 Rate-Dependent Ballistic Response of PMMA.....	7
3.4 Compression Measurements of Monolithic PMMA and PC	9
3.5 PC-Glass-PMMA-PC Laminates	11
3.6 Ballistic Measurements Against the 9-mm Projectile	14
4. Conclusions	16
5. References	17
Distribution List	18

List of Figures

Figure 1. Pictures of .22-cal. FSP (left) and 124-gr, 9-mm projectile (right).....	4
Figure 2. V_{50} values obtained for the PC-PMMA-PC and PC-PC-PC laminates against the .22-cal. FSP impact.....	5
Figure 3. Typical fracture pattern of the PC-PMMA-PC laminate after impact with the .22-cal. FSP.....	6
Figure 4. Typical fracture pattern of the PC-PC-PC laminate after impact with the .22-cal. FSP.....	6
Figure 5. Typical conoid fracture pattern observed in the exit side of the PC-PMMA-PC laminate after impact with the .22-cal. FSP.....	7
Figure 6. V_{50} values obtained for the PMMA-Sim PU laminates against the .22-cal. FSP impact.....	8
Figure 7. Plot of V_{50} vs. areal density for the PC-PMMA-PC, PMMA-Sim 2003 PU, and PMMA-PC laminates against the .22-cal. FSP impact.....	8
Figure 8. Plot of V_{50} vs. nominal plate thickness of monolithic PMMA and PC against the .22-cal. FSP impact.....	9
Figure 9. Brittle mode cracking compared to localized deformation observed in the 6-mm thick monolithic PMMA after impact with the .22-cal. FSP at a velocity of (a) 173 m/s and (b) 1004 m/s, respectively.....	10
Figure 10. Plots of ballistic energy values as a function of striking velocity obtained for the monolithic PMMA of various target thicknesses against the .22-cal. FSP impact; inserts show the corresponding mode of impact-induced failure; solid lines are the second-order polynomial curve fit for the corresponding data.....	10
Figure 11. Plots of stress vs. strain data obtained from the constant-strain rate compression measurements at 0.001/s and 1/s for the monolithic PMMA and PC.....	11
Figure 12. Comparison of the apparent compressive yield strength of PC and PMMA with respect to the strain rate.....	12
Figure 13. Plot of V_{50} vs. areal density data for the PC-Glass-PMMA-PC laminates (listed in table 4) against the .22-cal. FSP impact.....	13
Figure 14. A combined plot of V_{50} vs. areal density data for the all-plastic laminates (figure 7) and PC-Glass-PMMA-PC laminates (figure 13) against the .22-cal. FSP impact; solid lines are the linear curve fit for the corresponding data.....	13
Figure 15. PC-PMMA-PC laminate after impact with the 9-mm projectile at 480 m/s.....	14
Figure 16. PC-PMMA-PC laminate after impact with the 9-mm projectile at 390 m/s.....	15
Figure 17. PC-PC-PC laminate after impact with the 9-mm projectile at 399 m/s.....	15
Figure 18. Comparison of the extent of residual visibility seen in the PC-PMMA-PC laminate (left) and PC-Glass-PMMA-PC laminate (right) after the 9-mm projectile impact.....	16

List of Tables

Table 1. Target configuration and areal density of plastic-based laminates obtained from GE Polymershapes.	2
Table 2. Target configuration and areal density of plastic-based laminates obtained from Protech Armor Products.	2
Table 3. Target configuration and areal density of PMMA-Sim polyurethane laminates.	2
Table 4. Target configuration and areal density of Pyrex glass-plastic laminates.	3
Table 5. Target configuration and areal density of sodalime glass-plastic laminates.	3
Table 6. Values of apparent compressive yield stress as a function of constant strain rate for the monolithic PMMA and PC.	12
Table 7. Areal density of PC-PMMA-PC and PC-Glass-PMMA-PC laminates and their corresponding V_{50} values against the 9-mm projectile.	14

Acknowledgments

The authors would like to thank Russell Prather and Ricky Kane of the U.S. Army Research Laboratory (ARL) for performing the ballistic testing and data acquisition, Dr. Walter Zukas at the Natick Soldier Center (NSC) for review and comments, Randy Natches at NSC for fabricating the compression test specimens, and Thomas Haines of GE Polymers for providing the PC (polycarbonate)-PMMA poly(methyl methacrylate)-PC and PC-PC-PC laminate samples.

1. Introduction

Recent events in Operation Iraqi Freedom reveal a critical demand for lightweight transparent armor with enhanced survivability against emerging threats. Thus, the U.S. Army Research Laboratory (ARL) is engaged in a joint effort with partners to further develop and optimize novel hybrid hard/ductile composites with capabilities of defeating a wider range of ballistic threats at higher mass efficiencies (i.e., reduced weights and thicknesses) and lower costs (*1*).

Transparent armor materials are commercially available and have been applied in a variety of military and civilian systems and equipment including face shields, goggles, vehicle vision blocks, windshields and windows, blast shields, and aircraft canopies. However, almost all reports that are available in the literature do not address whether material characteristics such as strain-rate sensitivity of the monolithic components is critical to the overall ballistic performance of these laminated armor systems. This research focuses on the transparent polymeric materials primarily used for personnel and ground vehicle protection. Earlier test results revealed that poly (methyl methacrylate) (PMMA) plays an important role in the ballistic optimization of laminated structures consisting of PMMA and polycarbonate (PC) (*2, 3*). PC is ductile in nature and serves as backing plates to mitigate spall-induced damage as well as to provide the desired structural support. The monolithic PMMA, albeit brittle upon the tensile deformation, exhibits better impact performance against the .22-cal. fragment simulator projectile (FSP) than PC at equivalent plate thickness ~ 12 mm or higher. These experimental findings provide the basis for materials selection, such as using thin monolith of ductile polymers for eye protection systems like goggles and visors, for optimization of layer configuration of composites utilized as ballistic shields for the Explosive Ordnance Disposal (EOD), and for potential vehicle applications.

One of the objectives of this research is to determine whether the unique impact behavior of PMMA is primarily geometry-dependent or if it is an intrinsic characteristic of the material. In this study, we have carried out ballistic measurements over a wide range of impact velocities including those well above the ballistic limits and determined the impact response of PMMA with respect to the loading conditions. We also evaluated the effect of PMMA plate thickness on the overall ballistic performance of the selected PC-PMMA-PC, PMMA-PC, PMMA-Simula (SIM) 2003 polyurethane, and glass-plastic systems. The work on glass-plastic laminates serves as the feasibility study to determine the effectiveness of integrating PMMA in the design and ballistic optimization of ceramic-plastic laminates-based armor. The preliminary test results obtained from the 9-mm projectile impact measurements for the selected laminate systems are also included for discussion.

2. Experimental

2.1 Target Materials

The selected laminates consisting of various layer configurations of monolithic plates of Lexan^{*} polycarbonate, and Plexiglas G[†] poly (methyl methacrylate), were prepared and obtained either from Protech Armor Products (Pittsfield, MA) or from GE Polymershapes (Allentown, PA). These laminates, with an overall plate thickness close to those of the EOD shields of interest, were selected as model materials systems for this study. Table 1 lists the plate configuration and areal density of the PC-PMMA-PC and PC-PC-PC laminates from GE Polymershapes, and table 2 lists the PMMA-PC laminates from the Protech Armor Products. The selected PMMA-Sim PU laminates listed in table 3, consisting of PMMA as front plate and Sim 2003 polyurethane (from Simula Technologies, Inc., Phoenix, AZ) as back plate, were also included for comparison.

Table 1. Target configuration and areal density of plastic-based laminates obtained from GE Polymershapes.

Target Type	Laminate Configuration	Areal Density (lb/ft ²)
PC-PMMA-PC	3-mm PC/12-mm PMMA ^a /3-mm PC	4.68
PC-PC-PC	3-mm PC/12-mm PC/3-mm PC	4.85

^a Nominal thickness of the cast PMMA plate.

Table 2. Target configuration and areal density of plastic-based laminates obtained from Protech Armor Products.

Target Type	Laminate Configuration	Areal Density (lb/ft ²)
PMMA-PC-1	12-mm PMMA ^a /3-mm PC	3.81
PMMA-PC-2	9-mm PMMA ^a /6-mm PC	3.82
PMMA-PC-3	12-mm PMMA ^a /6-mm PC	4.37
PMMA-PC-4	18-mm PMMA ^a /3-mm PC	5.25
PMMA-PC-5	18-mm PMMA ^a /6-mm PC	5.59

^a Nominal thickness of the cast PMMA plate.

Table 3. Target configuration and areal density of PMMA-Sim polyurethane laminates.

Target Type	Laminate Configuration	Areal Density (lb/ft ²)
PMMA-Sim 2003 PU-1	6-mm PMMA ^a /6-mm Sim 2003 PU	3.18
PMMA-Sim 2003 PU-2	9-mm PMMA ^a /6-mm Sim 2003 PU	3.85

^a Nominal thickness of the cast PMMA plate.

^{*} Lexan is a registered trademark of General Electric Co.

[†] Plexiglas G is a registered trademark of ATOFINA Chemicals, Inc.

Two sets of glass-plastic targets were prepared—Pyrex* glass was used in one set and soda lime glass in the other; both were acquired from Swift Glass Company, Inc. (Elmira, NY). These glass-plastic targets were not bonded with any adhesives, but instead stacked together and wrapped tightly with heavy gauge construction tape around the sides. This practice serves well for the preliminary evaluation as well as for the ease of disassemble of targets in order to examine the damage associated with each plate from the impact. Tables 4 and 5 list the target configuration and the areal density of these glass-plastic laminates with Pyrex glass and soda lime glass, respectively.

Table 4. Target configuration and areal density of Pyrex glass-plastic laminates.

Target Type	Laminate Configuration	Areal Density (lb/ft ²)
PC-Glass-PMMA-PC-1	1.5-mm PC/2.5-mm glass/6-mm PMMA ^a /1.5-mm PC	3.53
PC-Glass-PMMA-PC-2	1.5-mm PC/2.5-mm glass/9-mm PMMA ^a /1.5-mm PC	4.30
PC-Glass-PMMA-PC-3	1.5-mm PC/2.5-mm glass/12-mm PMMA ^a /1.5-mm PC	5.08

^a Nominal thickness of the cast PMMA plates.

Table 5. Target configuration and areal density of sodalime glass-plastic laminates.

Target Type	Laminate Configuration	Areal Density (lb/ft ²)
PC-Glass-PMMA-PC-1	3-mm PC/3-mm glass/9-mm PMMA ^a /3-mm PC	5.14
PC-Glass-PMMA-PC-2	3-mm PC/3-mm glass/12-mm PMMA ^a /3-mm PC	5.92

^a Nominal thickness of the cast PMMA plates.

2.2 Ballistic Testing

The ballistic measurements were carried out at ARL Experimental Facility Peep Sight Range 20 at Aberdeen Proving Ground, MD, primarily using the 17-gr (1.1-g weight), .22-cal. FSP and, in some cases, with the 124-gr full-metal-jacket 9-mm projectile (figure 1). The target laminates were C-clamped at all four corners to the backside of a heavy steel test stand; the stand had a 12 mm-diameter opening in the center. For the .22-cal. FSP, the testing was conducted using a 0.56-m-long, 5.66-mm barrel with a 1:12 twist. For the 9-mm tests, a 9-mm Mann barrel with a 1:9.75 twist was used. The muzzle of the gun was placed 2.5 m from the target fixture. All shots were conducted with the target normal to the projectile line of flight, i.e., 0° obliquity. During the ballistic measurements, the amount of smokeless powder that was loaded into the brass case was varied to control the projectile velocity. Specimens were subjected to impact over a range of

* Pyrex is a registered trademark of Corning.



Figure 1. Pictures of .22-cal. FSP (left) and 124-gr, 9-mm projectile (right).

striking velocities in order to achieve complete penetration and partial penetration. The ballistic limit, commonly referred to as V_{50} , is a statistical value and is regarded as the velocity at which the projectile has a 50% chance of perforating the target at normal incidence of impact. In this study, at least eight test specimens of each composition were used for the ballistic measurements, except in the cases where only a limited number of target specimens was available for testing. All shots were examined for pitch, yaw, and total yaw to ensure a fair test. The V_{50} value was determined from the averaging of the lowest impact-velocity values, in which target specimens failed in complete penetration, and the highest velocity values associated with partial penetration. The spread between the impact velocity values associated with complete and partial penetration is within 38 m/s, following the guideline of the MIL-STD-662F specifications (4). In some cases, in addition to the V_{50} measurement, the ballistic impact energy exerted on the target was calculated based on the change of kinetic energy of the projectile before and after the penetration into the target, as shown in equation 1. The mass (M) of the projectile is assumed unchanged during the impact.

$$\text{Ballistic energy} = 1/2 M (V_s^2 - V_r^2), \quad (1)$$

where V_s and V_r are the striking and residual velocities, respectively.

2.3 Compression Measurements

Quasistatic compression measurements of the monolithic PMMA and PC were performed by using the Instron model 1331 testing machine. Cylindrical shape specimens of 6-mm diameter with a 3-mm gauge length, yielding a diameter to depth ratio of 2:1, were selected. True strain-controlled compression testing was used at a constant-strain rate ranging from 0.001/s to 1/s; this mode was achieved with the use of a programmable function generator providing the command signal source to the auxiliary input of the Instron controller. Liberal amounts of a lubricant were applied to the specimen to minimize friction between the specimen ends and platens during the compression measurements.

3. Results and Discussion

We have examined the role of PMMA on the overall ballistic performance of the PC-PMMA-PC, PMMA-PC, PMMA-Sim PU, and PC-glass-PMMA-PC systems, and will discuss the test results in the following sections.

3.1 PC-PMMA-PC vs. PC-PC-PC Laminates

The details of layer configuration and areal density of these laminates are listed in table 1. The PC-PMMA-PC laminates exhibit a 37% higher value of the V_{50} when compared with the PC-PC-PC laminates of equivalent overall layer configuration against the .22-cal. FSP impact (figure 2). These results are consistent with the earlier experimental observations; the PC-PMMA-PC laminates are more effective than the corresponding all-PC laminates, despite the fact that monolithic PC is ductile upon impact. The failure mechanisms associated with these two laminates are distinctly different; the all-PC laminates display localized plug failure with damage limited to the immediate vicinity of impact (figure 3), while radial and circumferential cracks form over the PMMA plate in the PC-PMMA-PC laminates (figure 4). A conoid fracture pattern (figure 5) is evident in the exit side of PMMA in the PC-PMMA-PC laminates, similar to the brittle fracture pattern observed in the typical hard ceramic systems. It is generally recognized that the extent in the spreading of impact energy is closely related to the ability to form a conoid shaped damage zone within the ceramic plate of the ceramic-metal composites armor. This fracture pattern is generally regarded as the major factor to the synergistic interaction between the brittle and ductile layers (5–7); however, it may not be the only attribute to the ballistic response of polymer-based hybrid composites.

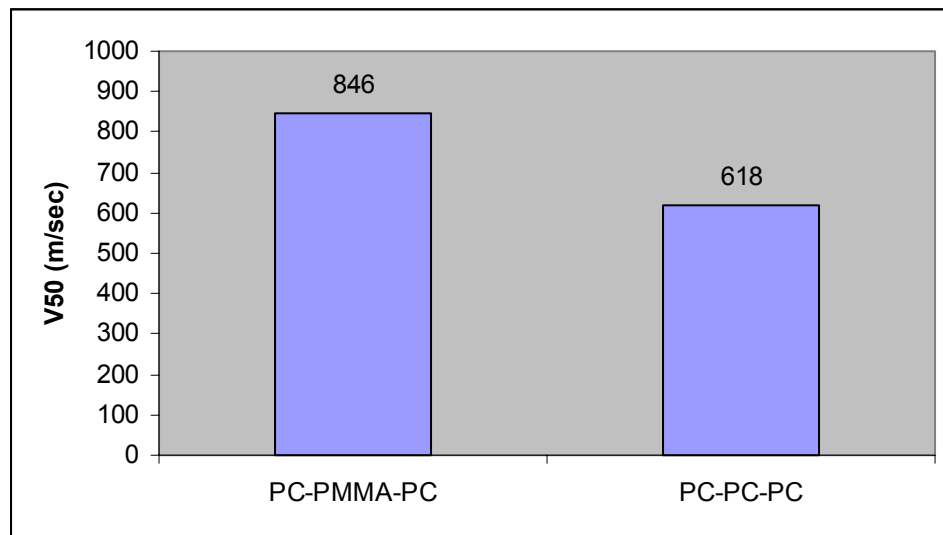


Figure 2. V_{50} values obtained for the PC-PMMA-PC and PC-PC-PC laminates against the .22-cal. FSP impact.



Figure 3. Typical fracture pattern of the PC-PMMA-PC laminate after impact with the .22-cal. FSP.

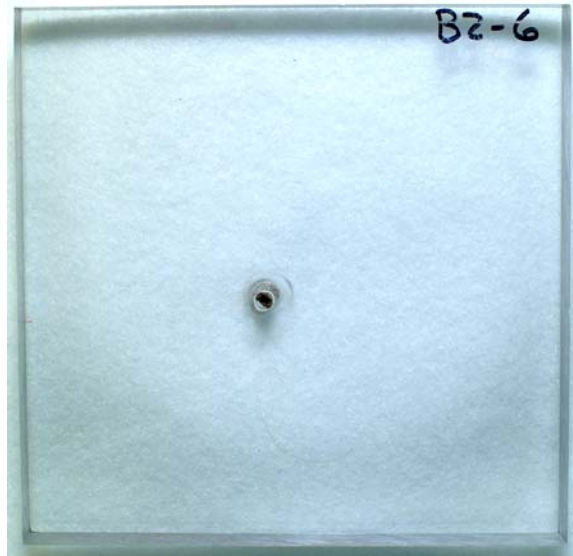


Figure 4. Typical fracture pattern of the PC-PC-PC laminate after impact with the .22-cal. FSP.



Figure 5. Typical conoid fracture pattern observed in the exit side of the PC-PMMA-PC laminate after impact with the .22-cal. FSP.

3.2 Effect of PMMA Plate Thickness

We examined the ballistic performance of laminates consisting of Simula polyurethane (PU), instead of PC, as a back support. The V_{50} value of the PMMA-Sim PU laminates increases with increasing PMMA plate thickness (8), as shown in figure 6. In order to validate the effectiveness of PMMA in the PMMA-Sim PU laminates vs. in the PC-PMMA-PC and PMMA-PC laminates (listed in table 2), we plot the V_{50} values as a function of areal density, since some of these laminates consist of different configurations. The V_{50} data shown in figure 7 appear to be directly proportional to the areal density regardless of the laminate configuration. It is noted that the variation of areal density reflects primarily the difference of the plate thickness of PMMA used in these laminates.

The velocity of stress wave propagation in a material is proportional to the square root value of Young's modulus divided by density; therefore, the stiffer PMMA is presumably more capable of dissipating the shock-induced stresses than the PC and Sim PU. The V_{50} data shown in figure 7 reveal that the use of PMMA to achieve the synergistic ballistic enhancement of hybrid hard/ductile composites is consistent in both PMMA-Sim PU and PC-PMMA-PC (including PMMA-PC) laminates. These results further suggest that PMMA is effective over the selected range of areal densities that are of interest for structural optimization for various armor applications.

3.3 Rate-Dependent Ballistic Response of PMMA

As mentioned earlier, the monolithic PMMA exhibited equal or better impact performance against the .22-cal. FSP impact than PC at a thickness ~ 12 mm or above, as shown in figure 8 (2, 3). We attempted to determine whether this unique impact behavior was merely target-geometry dependent or if it was indeed characteristic of PMMA. We carried out the ballistic

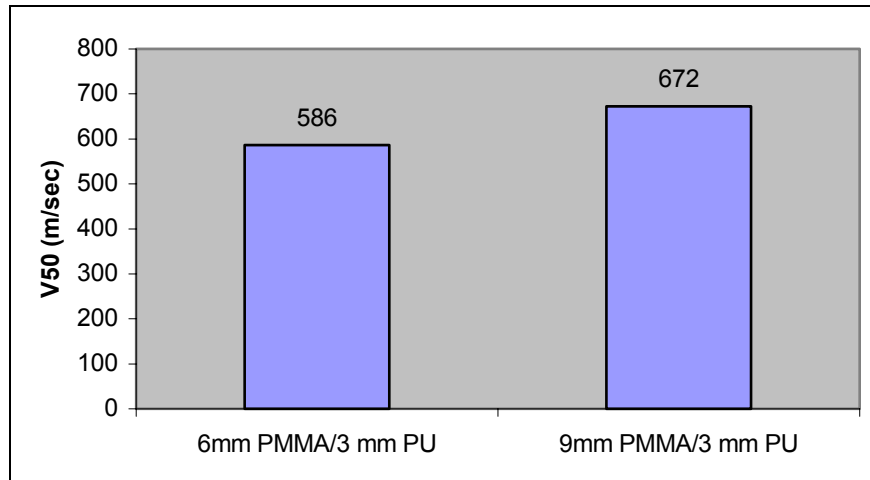


Figure 6. V_{50} values obtained for the PMMA-Sim PU laminates against the .22-cal. FSP impact.

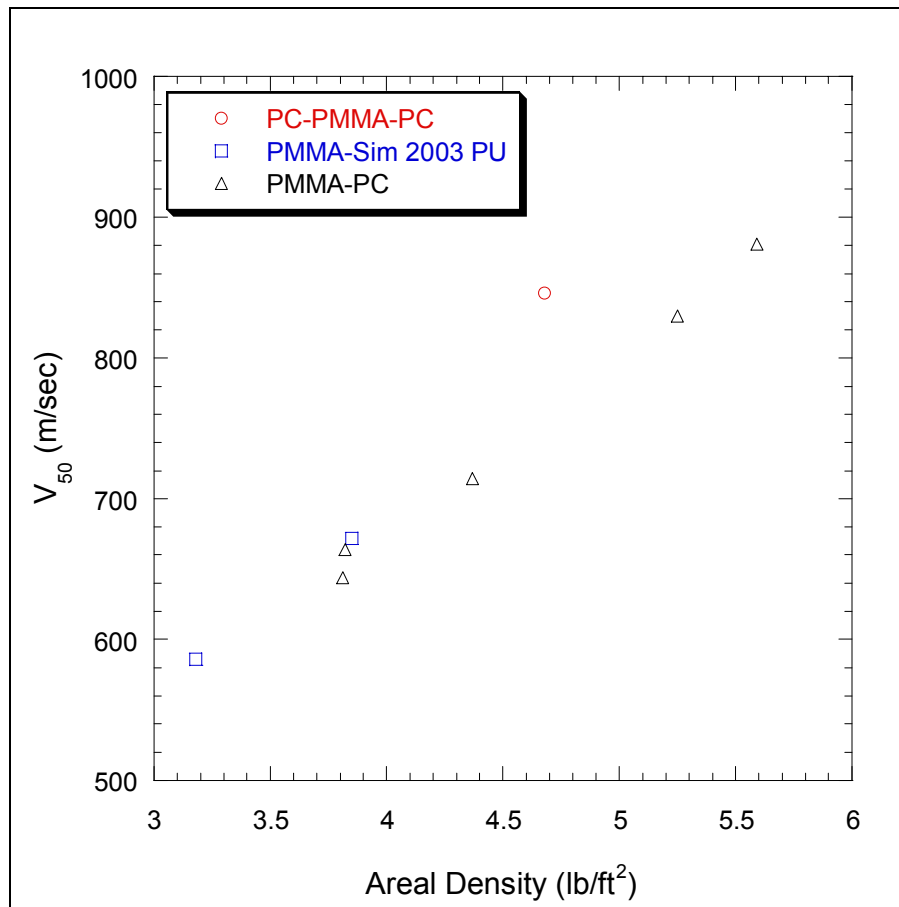


Figure 7. Plot of V_{50} vs. areal density for the PC-PMMA-PC, PMMA-Sim 2003 PU, and PMMA-PC laminates against the .22-cal. FSP impact.

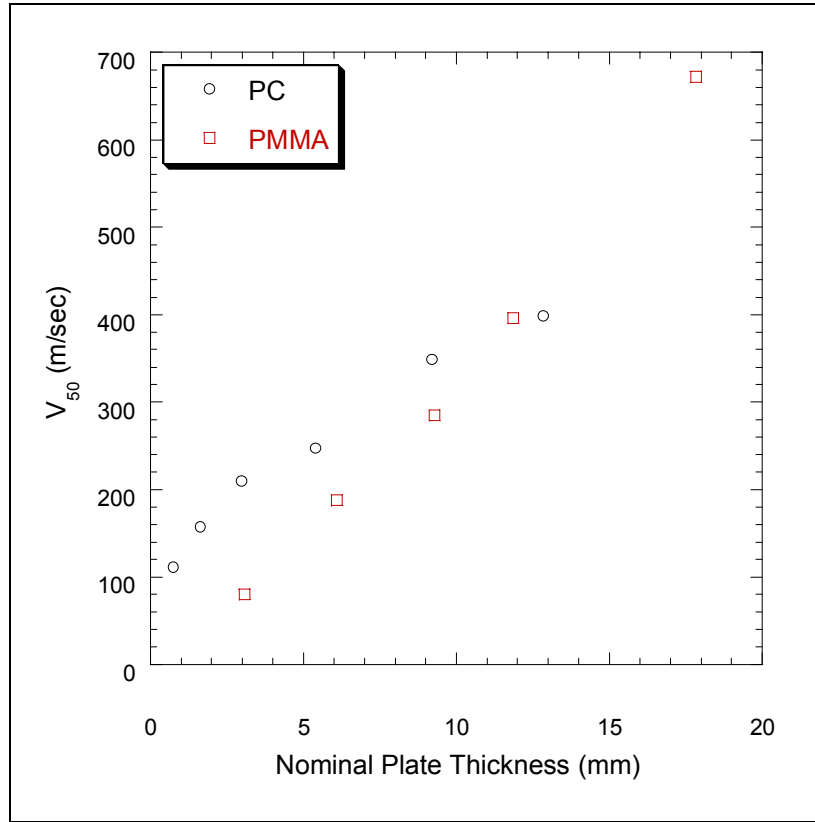


Figure 8. Plot of V_{50} vs. nominal plate thickness of monolithic PMMA and PC against the .22-cal. FSP impact.

testing of PMMA of various plate thicknesses at impact velocities in the range of 200 m/s to 1300 m/s, well above their V_{50} values. PMMA exhibited a change of mode of failure from brittle type cracking to more localized deformation as the impact velocity increases; figures 9a and 9b are the representative photographs displaying the corresponding fracture patterns. The apparent ballistic energy values were also calculated using equation 1 and were plotted as a function of striking velocity in figure 10 for the 6, 9, and 12-mm thick PMMA targets. It is evident that the ballistic energy value increases with increasing impact velocity, which corresponds to the observation of brittle-to-ductile transition of PMMA with respect to the increase of impact velocity (see inserts in figure 10).

3.4 Compression Measurements of Monolithic PMMA and PC

Quasistatic compression testing was carried out to validate the rate-dependent ballistic response of PMMA. Measurements of the true stress vs. true strain of the monolithic PMMA and PC under compression were conducted at a constant strain rate ranging from 0.001/s to 1/s (9, 10). Results in figure 11 show that PMMA, albeit brittle upon the tensile deformation, displays



Figure 9. Brittle mode cracking compared to localized deformation observed in the 6-mm thick monolithic PMMA after impact with the .22-cal. FSP at a velocity of (a) 173 m/s and (b) 1004 m/s, respectively.

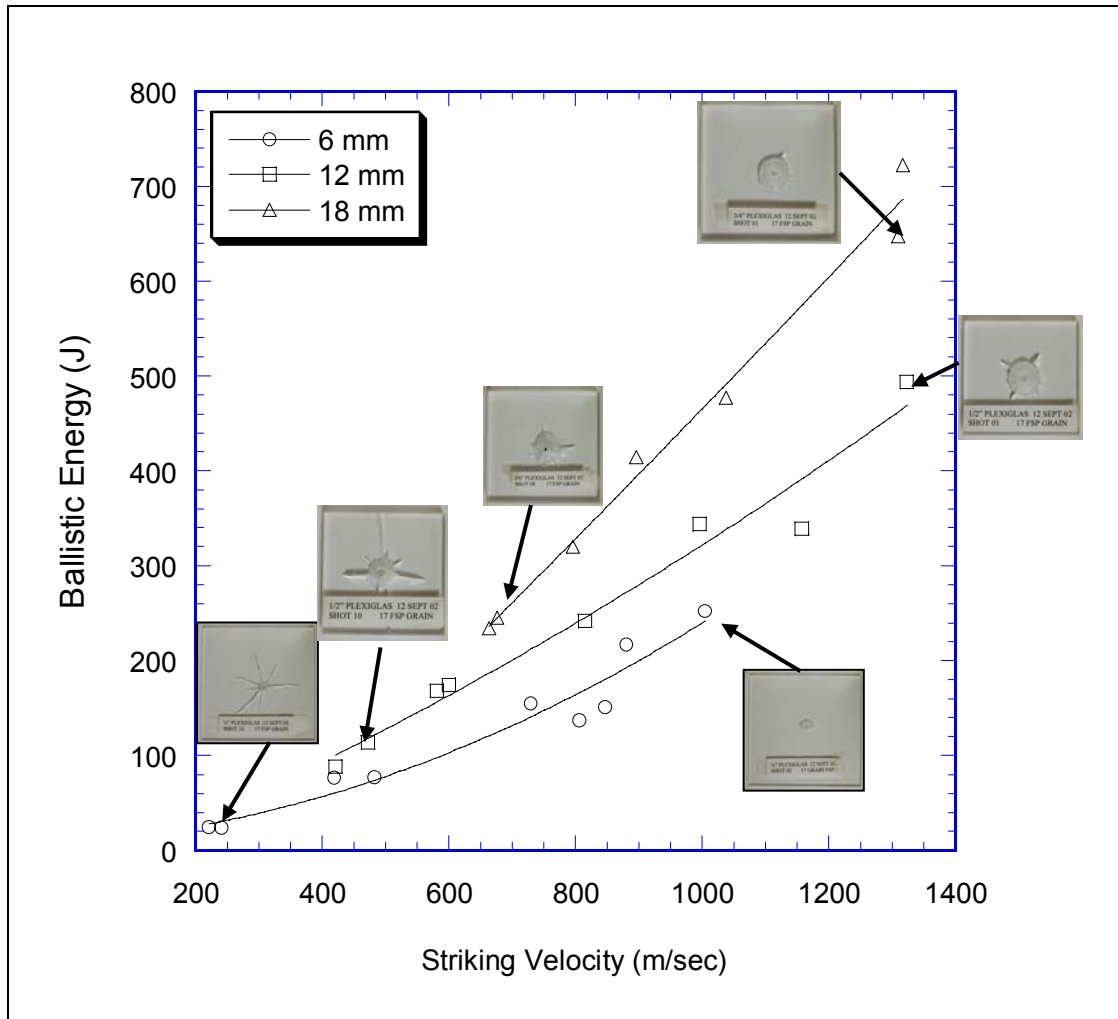


Figure 10. Plots of ballistic energy values as a function of striking velocity obtained for the monolithic PMMA of various target thicknesses against the .22-cal. FSP impact; inserts show the corresponding mode of impact-induced failure; solid lines are the second-order polynomial curve fit for the corresponding data.

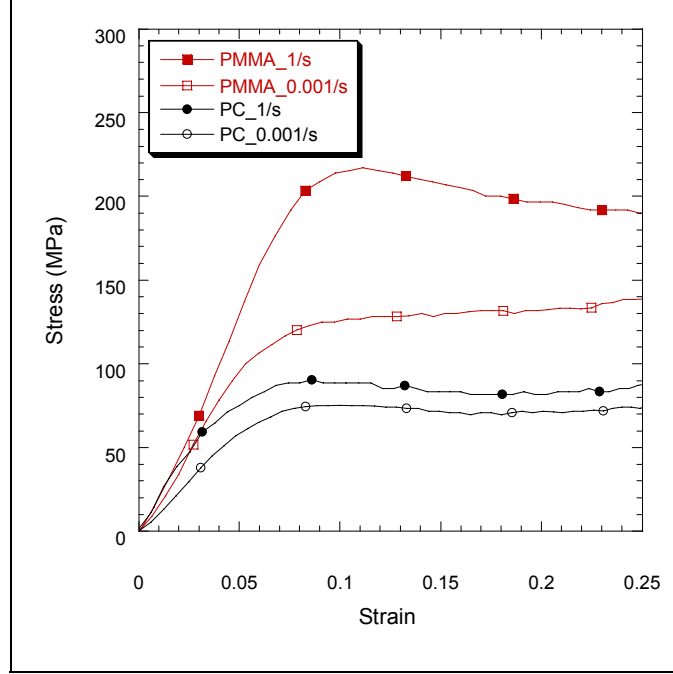


Figure 11. Plots of stress vs. strain data obtained from the constant-strain rate compression measurements at 0.001/s and 1/s for the monolithic PMMA and PC.

elastic-plastic deformation with an initial viscoelastic response followed by yielding, strain softening, and strain hardening in compression, similar to PC. The apparent yield stress of PMMA is much higher than that of PC. Furthermore, PMMA exhibits higher rate-sensitivity than PC; the increase of apparent yield stress with respect to the strain rate is much more significant in PMMA than in PC (figure 12). Table 6 lists the values of apparent compressive yield stress of PMMA and PC.

3.5 PC-Glass-PMMA-PC Laminates

Despite the fact that the state of the stress encountered at high impact velocities is very complicated, we hypothesized that the high strain-rate sensitivity characteristics of PMMA were its intrinsic material response. Furthermore, we exploited this observation to the practical use in the design and system optimization of transparent armor. For example, we incorporated PMMA as an additional intermediate ply within the typical glass-PC laminates in order to determine whether PMMA was effective in the PC-Glass-PMMA-PC laminate systems. As stated earlier, instead of using adhesive bonding, we stacked these plates together and wrapped them tightly with construction tape around the sides for preliminary evaluation. Figure 13 plots the V_{50} values as a function of areal density obtained for the PC-Glass-PMMA-PC laminates against the .22-cal. FSP impact. The variation of area density reflects the difference of the plate thickness of PMMA used in these laminates listed in table 4; it is evident that the ballistic impact performance improves with incorporation of thicker PMMA plates. Figure 14 compares these

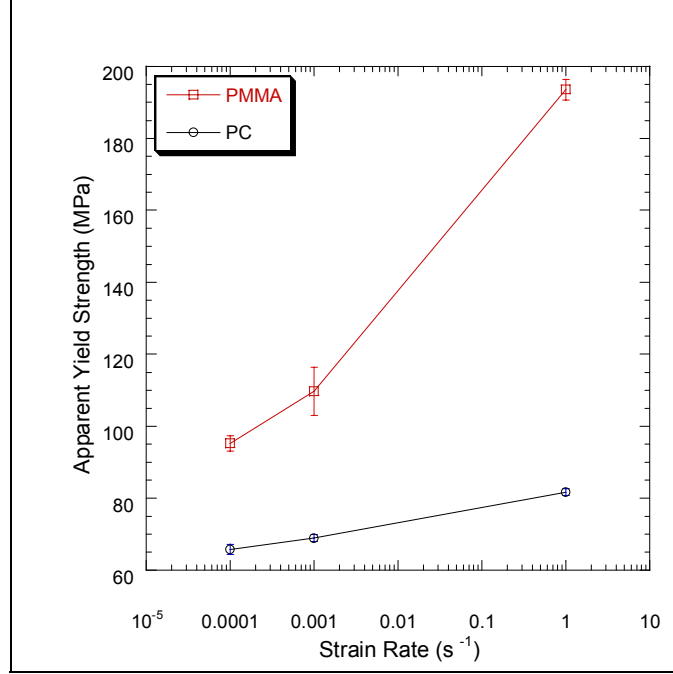


Figure 12. Comparison of the apparent compressive yield strength of PC and PMMA with respect to the strain rate.

Table 6. Values of apparent compressive yield stress as a function of constant strain rate for the monolithic PMMA and PC.

Constant Strain Rate (s ⁻¹)	Apparent Compressive Yield Stress (MPa)	
	PMMA	PC
10 ⁻⁴	95.2 ± 2.1	65.8 ± 1.3
10 ⁻³	109.7 ± 6.6	68.9 ± 1.0
1	193.5 ± 2.8	81.7 ± 1.0

data with all the V_{50} vs. areal density data available for the all-plastic laminates shown in figure 7; the solid lines are the linear curve-fit of these data. It is apparent that the effect of PMMA plate thickness on the overall ballistic performance is more significant in the glass-plastic laminates than in the all-plastic laminates. Incorporating PMMA as intermediate ply between the glass and ductile PC presumably can provide better impedance match and subsequently facilitate the shock wave propagation throughout the glass-PMMA-PC systems than the corresponding laminates without PMMA. We also attribute the observation of the overall impact enhancement to the high strain-rate sensitivity characteristics of the monolithic PMMA, seen in figure 10, due to the fact that these glass-plastic laminates with increasing PMMA plate thickness encountered much higher impact velocities upon the V_{50} measurements. These results validate our intent to integrate PMMA into the design of ceramic-plastic-based armor for protection against emerging threats.

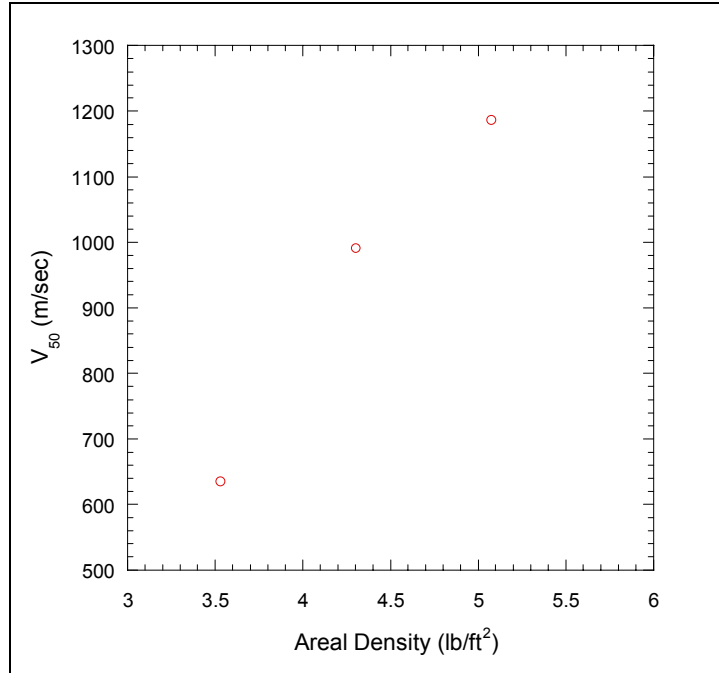


Figure 13. Plot of V_{50} vs. areal density data for the PC-Glass-PMMA-PC laminates (listed in table 4) against the .22-cal. FSP impact.

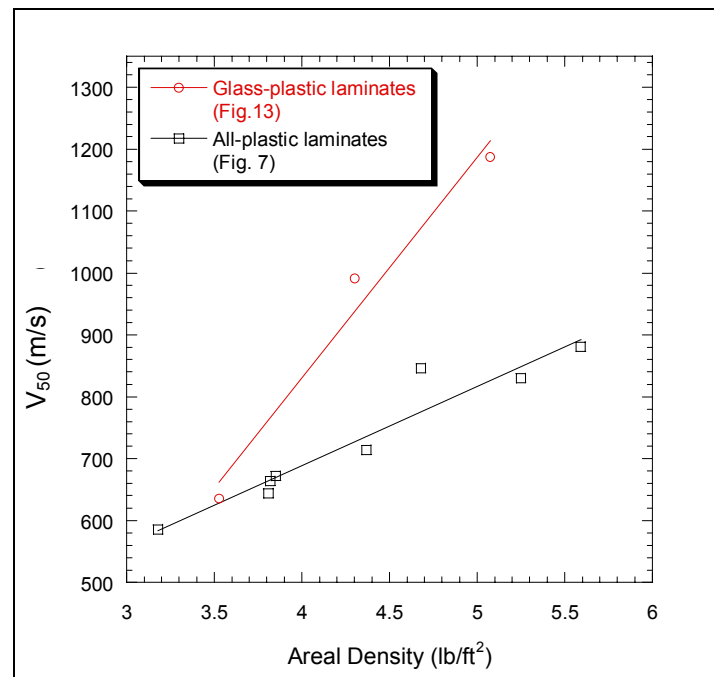


Figure 14. A combined plot of V_{50} vs. areal density data for the all-plastic laminates (figure 7) and PC-Glass-PMMA-PC laminates (figure 13) against the .22-cal. FSP impact; solid lines are the linear curve fit for the corresponding data.

3.6 Ballistic Measurements Against the 9-mm Projectile

We have conducted the preliminary ballistic evaluation of selected laminate systems against the 9-mm projectile. Table 7 summarizes the overall target configuration, areal density, and V_{50} values of PC-PMMA-PC, PC-PC-PC, and PC-Glass-PMMA-PC laminates (listed in table 5). The first two sets are all-plastic laminates with similar configuration (table 1); the PC-PMMA-PC laminates nevertheless show better V_{50} (477 m/s) than the corresponding PC-PC-PC laminates (385 m/s). In addition, the PC-PMMA-PC laminates appear to be able to break the 9-mm projectile apart during impact; figures 15 and 16 display the damaged projectile resulting from impact at a velocity of 480 m/s or even well below V_{50} at 390 m/s, respectively. The PC-PC-PC laminate, on the other hand, only deforms but does not cause rupture of the 9-mm projectile, as shown in figure 17.

The glass-plastic laminates consisting of 12-mm thick PMMA withstood the 9-mm projectile impact without complete penetration. The PC-PMMA-PC laminates with similar overall thickness as the PC-Glass (3-mm thick)-PMMA (9-mm thick)-PC laminates are about 9% lighter in terms of areal density, yet exhibit only about 6% difference in V_{50} (477 m/s vs. 507 m/s).

Table 7. Areal density of PC-PMMA-PC and PC-Glass-PMMA-PC laminates and their corresponding V_{50} values against the 9-mm projectile.

Laminate Configuration	Areal Density (lb/ft ²)	V_{50} (m/s)
3-mm PC/12-mm PC/3-mm PC	4.85	385
3-mm PC/12-mm PMMA ^a /3-mm PC	4.68	477
3-mm PC/3-mm Glass/9-mm PMMA ^a /3-mm PC	5.14	507
3-mm PC/3-mm Glass/12-mm PMMA ^a /3-mm PC	5.92	^b

^a Nominal thickness of the cast PMMA plate.

^b No complete penetration.

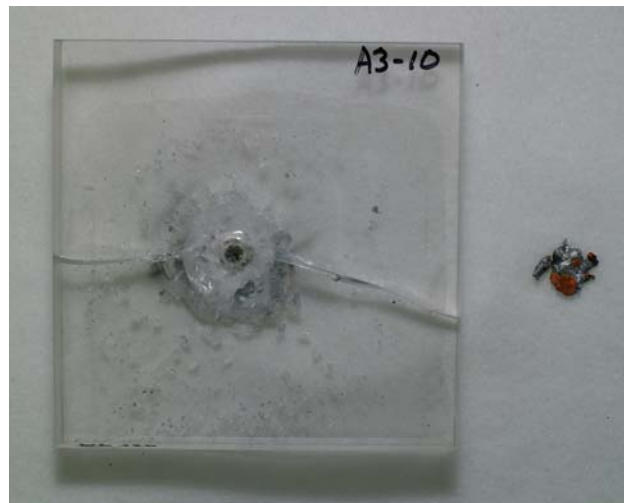


Figure 15. PC-PMMA-PC laminate after impact with the 9-mm projectile at 480 m/s.



Figure 16. PC-PMMA-PC laminate after impact with the 9-mm projectile at 390 m/s.



Figure 17. PC-PC-PC laminate after impact with the 9-mm projectile at 399 m/s.

Moreover, the PC-PMMA-PC laminates have significantly better residual visibility than the glass-plastic laminates, as shown in figure 18. These preliminary results serve as the basis for the further optimization studies and demonstrate that PMMA is effective and has potential as a replacement for glass in the design of glass-containing armor systems.



Figure 18. Comparison of the extent of residual visibility seen in the PC-PMMA-PC laminate (left) and PC-Glass-PMMA-PC laminate (right) after the 9-mm projectile impact.

4. Conclusions

We have evaluated the role of PMMA on the ballistic impact performance of the selected all-plastic- and glass-plastic-based laminates. Results show that the ballistic limit against the .22-cal. FSP increased with increasing plate thickness of PMMA in these targets. Based on the preliminary results, the effectiveness of PMMA against the .22-cal. FSP is also evident when testing against the 9-mm projectile. These experimental findings suggest that PC-PMMA-PC or other all-plastic laminates are the systems of choice, particularly for incorporation into the design of vehicle transparent armor applications. We are currently undertaking this approach to determine the ballistic response with respect to the target thickness for the monolithic PMMA, PC, and Sim PUs to better understand the interaction between the projectile and each individual component in order to best optimize the overall target requirements against the 9-mm threats.

5. References

1. McCauley, J.; Parimal, P.; Gilde, G.; Dehmer, P. G.; Hsieh, A. J. *Transparent Armor Systems*; brochure; U.S. Army Research Laboratory: Aberdeen Proving Ground, MD, June 2002.
2. Hsieh, A. J.; Song, J. W. The Role of PMMA in Ballistic Impact Response of Hybrid Hard/Ductile Composites. In preparation for *Polymer Composites*, 2003.
3. Song, J. W.; Hsieh, A. J. Ballistic Impact Resistance of Monolithic, Hybrid and Nano Composites of PC and PMMA. *Proceedings of the 17th American Society for Composites Technical Conference*, Purdue University, West Lafayette, IN, October 2002.
4. MIL-STD-662F. *V50 Ballistic Test for Armor* **1977**.
5. Florence, A. J. *Interaction of Projectiles and Composite Armor*; AMMRC-CR-69-15; Army Materials and Mechanics Research Center: Watertown, MA, August 1969.
6. Hetherington, J. G. The Optimization of Two Component Composite Armours. *Int. J. Impact Energy* **1992**, *12*, (3), 409–414.
7. Hetherington, J. G.; Rajagopalan, B. P. An Investigation Into the Energy Absorbed During Ballistic Perforation of Composite Armours. *Int. J. Impact Energy* **1991**, *11*, 33–40.
8. Dehmer, P. G. Weapons and Materials Research Directorate Personnel Protection Work Area program review; U.S. Army Research Laboratory: Aberdeen Proving Ground, MD, 2002.
9. Moy, P.; Weerasooriya, T.; Hsieh, A. J.; Chen, W. Strain Rate Response of a Polycarbonate Under Uniaxial Compression. *Proceedings of the SEM Annual Conference on Experimental Mechanics*, Charlotte, NC, June 2003.
10. Moy, P.; Weerasooriya, T.; Chen, W.; Hsieh, A. J. Dynamic Stress-Strain Response and Failure Behavior of PMMA. *Proceedings of the ASME International Mechanical Engineering Conference*, Washington, DC, November 2003.

NO. OF
COPIES ORGANIZATION

1
(PDF
Only) DEFENSE TECHNICAL
INFORMATION CTR
DTIC OCA
8725 JOHN J KINGMAN RD
STE 0944
FT BELVOIR VA 22060-6218

1 COMMANDING GENERAL
US ARMY MATERIEL CMD
AMCRDA TF
5001 EISENHOWER AVE
ALEXANDRIA VA 22333-0001

1 INST FOR ADVNCD TCHNLGY
THE UNIV OF TEXAS
AT AUSTIN
3925 W BRAKER LN STE 400
AUSTIN TX 78759-5316

1 US MILITARY ACADEMY
MATH SCI CTR EXCELLENCE
MADN MATH
THAYER HALL
WEST POINT NY 10996-1786

1 DIRECTOR
US ARMY RESEARCH LAB
AMSRD ARL D
DR D SMITH
2800 POWDER MILL RD
ADELPHI MD 20783-1197

1 DIRECTOR
US ARMY RESEARCH LAB
AMSRD ARL CS IS R
2800 POWDER MILL RD
ADELPHI MD 20783-1197

3 DIRECTOR
US ARMY RESEARCH LAB
AMSRD ARL CI OK TL
2800 POWDER MILL RD
ADELPHI MD 20783-1197

3 DIRECTOR
US ARMY RESEARCH LAB
AMSRD ARL CS IS T
2800 POWDER MILL RD
ADELPHI MD 20783-1197

NO. OF
COPIES ORGANIZATION

ABERDEEN PROVING GROUND

2 DIR USARL
AMSRD ARL CI LP (BLDG 305)
AMSRD ARL CI OK TP (BLDG 4600)